



**HAL**  
open science

## Monitoring of the creep and the relaxation behaviour of concrete since setting time, part 1: compression

Claude Boulay, Michela Crespini, Brice Delsaute, Stéphanie Staquet

### ► To cite this version:

Claude Boulay, Michela Crespini, Brice Delsaute, Stéphanie Staquet. Monitoring of the creep and the relaxation behaviour of concrete since setting time, part 1: compression. Strategies for Sustainable Concrete Structures, May 2012, France. 10p. hal-00875238

**HAL Id: hal-00875238**

**<https://hal.science/hal-00875238>**

Submitted on 21 Oct 2013

**HAL** is a multi-disciplinary open access archive for the deposit and dissemination of scientific research documents, whether they are published or not. The documents may come from teaching and research institutions in France or abroad, or from public or private research centers.

L'archive ouverte pluridisciplinaire **HAL**, est destinée au dépôt et à la diffusion de documents scientifiques de niveau recherche, publiés ou non, émanant des établissements d'enseignement et de recherche français ou étrangers, des laboratoires publics ou privés.

---

# Monitoring of the creep and the relaxation behaviour of concrete since setting time, part 1: compression



Aix-en-Provence, France

May 29-June 1, 2012

C. Boulay<sup>1</sup>, M. Crespini<sup>1</sup>, B. Delsaute<sup>2</sup>, S. Staquet<sup>2</sup>

<sup>1</sup>IFSTTAR-Paris, Paris East University, France

<sup>2</sup> Université Libre de Bruxelles (ULB), BATir – Brussels, Belgium

---

## 1. Introduction

Early age deformations of concrete are involved in cracking which can lead to service life reduction. In particular, the development of the concrete autogenous shrinkage under restrained conditions can lead to durability problems in concrete structures.

Numerous parameters are involved in the cracking process. An approach “from material to structures” implies the knowledge of experimental parameters and the use of models and numerical computations taking into account couplings between thermal, hydrous and mechanical behaviours of the material at early age. Such an approach contributes to a more realistic vision of the behaviour of a structure. Not only the evolution of the autogenous shrinkage, the thermal deformations, the CTE (coefficient of thermal expansion), the tensile and compressive strengths, the E-modulus and the Poisson’s ratio are needed but creep and relaxation in tension and in compression must also be taken into account for realistic numerical simulations purposes of the stress field.

A partnership between IFSTTAR and ULB allowed joined experimental tests on the same material (ordinary concrete) in order to investigate the early age mechanical behaviour since setting time. The compressive and tensile strength, the heat released, the ultrasonic pulse velocity (UPV), the Poisson’s ratio of this material were characterized. Together with these parameters, this paper (part 1& 2) presents an experimental methodology using two different test rigs enabling a monitoring of the stiffness, the creep or the relaxation of a concrete sample since setting time. Tension and compressive tests realized on a revisited Temperature Stress Testing Machine TSTM [1] at ULB are presented in a second part while compressive tests, realized on another test rig called BTJASPE [2] designed at IFSTTAR, are presented in the first one. In each part, rheological models are used for the description of the experimental set of data. The purpose of this study is to investigate the question of the equivalence between the early age creep and relaxation behaviour of concrete in tension and in compression for a typical reference ordinary concrete in sealed conditions.

BTJASPE is a test rig which enables early age compressive loadings on cylinders. Samples are cast inside a stainless steel mould (sealed conditions) around which a flow of water allows the control of the sample’s temperature. The Young’s modulus, the creep or the relaxation of the sample can be monitored at early age. Cyclic loadings are applied at regular intervals. In each cycle, a loading, controlled in displacement is applied, then the stress, or the strain, is kept constant during a short period and the sample is unloaded to a zero stress until the next cycle. The creep recovery can also be monitored under this null state of stress. Rheological functions are used to model the observations performed in compression. Results are expressed, after the setting time.

## 2. Test setup

### 2.1 Material ID

The mixture proportions of the ordinary concrete under focus are given in the Table 1.

Components	Mass (kg /m <sup>3</sup> )
CEMI 52.5 N PMES CP2	340
Sand (Bernières 0/4)	739
Gravel (Bernières 8/22)	1072
Total water	184

Table 1 - Mixture proportions of the concrete. The water to cement ratio is equal to 0.54.

This concrete has been characterized at early age and later ages. In particular, the strength development in compression and in tension (axial splitting test) and the Young's modulus in compression are given here (fig. 1 and 2). Temperature measurements and knowledge of the concrete activation energy ( $E_a = 32220 \text{ J mol}^{-1}$ ) made it possible to express the results in equivalent age (reference temperature = 20 °C). It can be added that, after the setting time, a very low value of the autogenous shrinkage has been observed, what it is not surprising at all since the W/C ratio is 0.54.

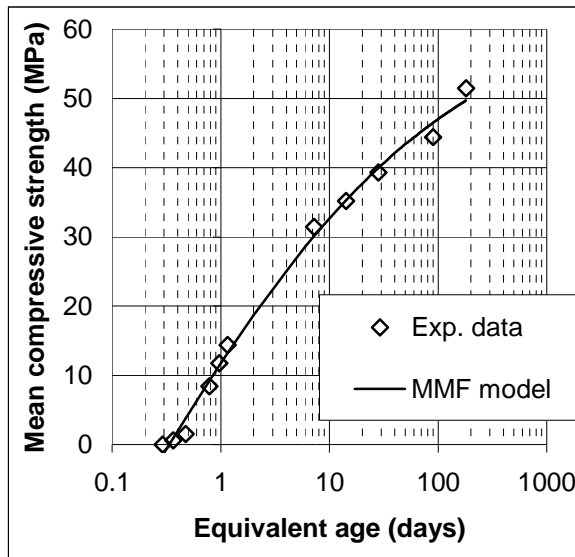


Fig. 1: Mean compressive strength modelled by a MMF [3] model:

$$f_{cm}(t) = \frac{a b + c t_{eq}^d}{b + t_{eq}^d}$$

( $a=83.9 \text{ MPa}$ ,  $b=0.56$ ,  $c=65.5 \text{ MPa}$  and  $d=0.3$ ).

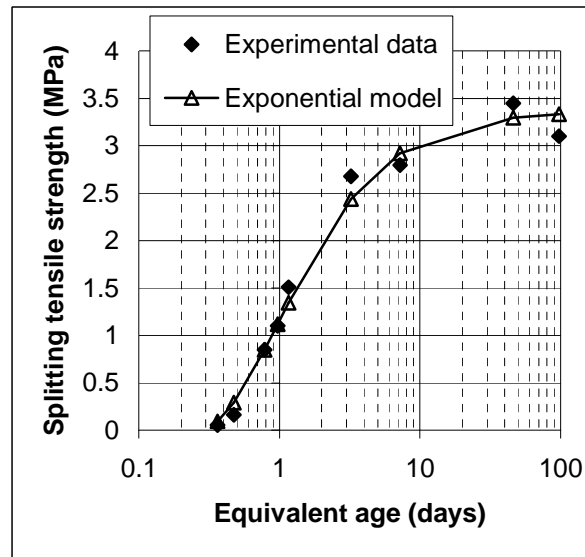


Fig. 2: Mean axial splitting strength modelled by the following function:

$$f_{ct, sp} = a \exp\left(-\frac{1}{t_{eq}}\right) - b$$

( $a = 3.5 \text{ MPa}$ ,  $b = 0,13 \text{ MPa}$ )

### 2.2 Experimental tools

A cylindrical concrete sample (100 mm in diameter, 200 mm in height) is cast inside a stainless steel mould (254 mm depth) whose thickness wall is 1 mm (fig. 5a). Before casting, the mould inner wall is greased. A circulation of water around the mould allows a perfect control of the sample temperature by the mean of an external circulator bath. Once the concrete is cast and placed, with a poker vibrator if necessary, it is levelled properly, approx. 50 mm under the edge of the mould, before installing a special upper bearing, guided inside the mould and equipped with supports for 3 LVDT's (fig. 5b).

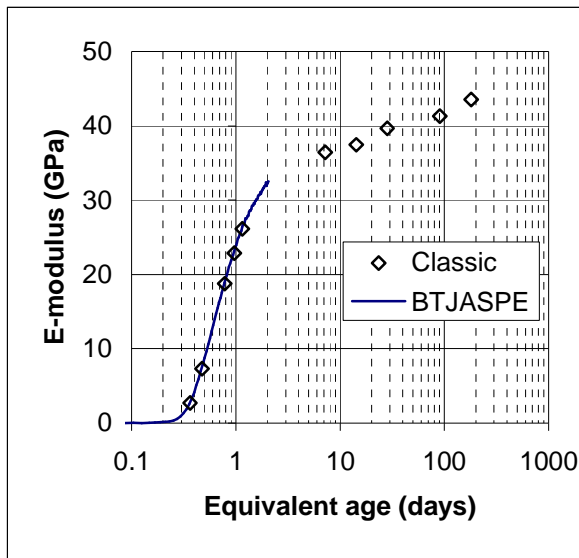


Fig. 3: E-modulus with manual measurements (classic) and automatic loadings [2]. These automatic loadings are obtained with a new apparatus and protocol described hereafter. Results are expressed in function of the compressive strength by a relation given in the figure 4.

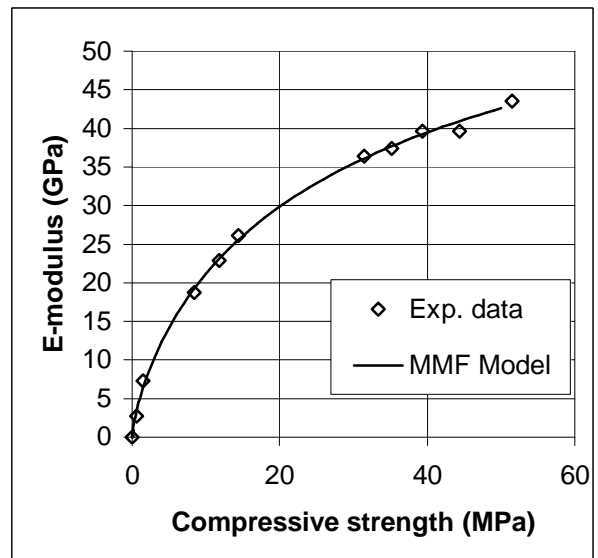


Fig. 4: Relation between the compressive strength and the E-modulus.

$$E = \frac{c f_{cm}^d}{b + f_{cm}^d}$$

( $c = 75000 \text{ MPa}$ ,  $d = 3/4$ ,  $b = 14.3 \text{ MPa}$ )

The rig is placed between the platens of a servo controlled testing machine. The upper loading tool, fixed under the load cell of the testing machine, is a cone inside which is located a system providing a measurement of the contact with the upper bearing placed upon the concrete sample (fig. 5c and 6). The lower bearing, fixed to the tip of the piston of the testing machine, is refreshed by a second circulation of water. A closed loop ensures a constant temperature of this bearing. Without this system, the heat coming from the oil of the machine is not properly evacuated and the temperature of the sample is largely affected (fig. 5 d).

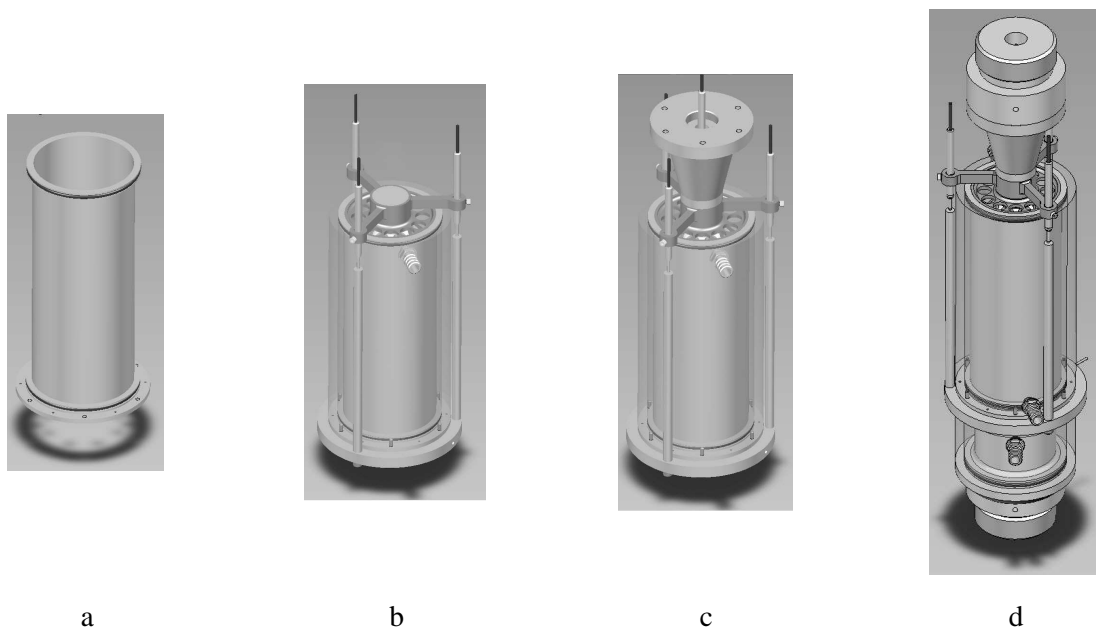


Fig. 5: The new test rig.

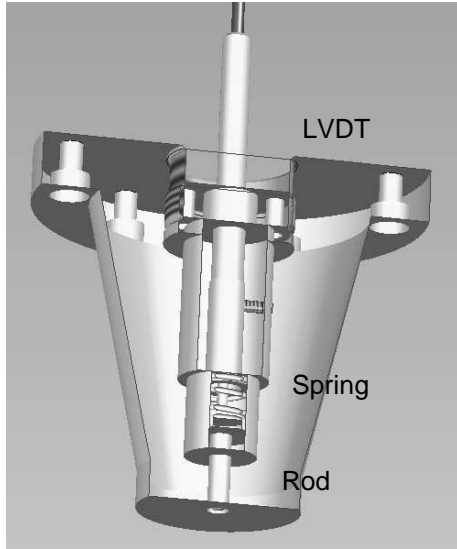


Fig. 6: Cut view (only contours) of the upper conical tool.

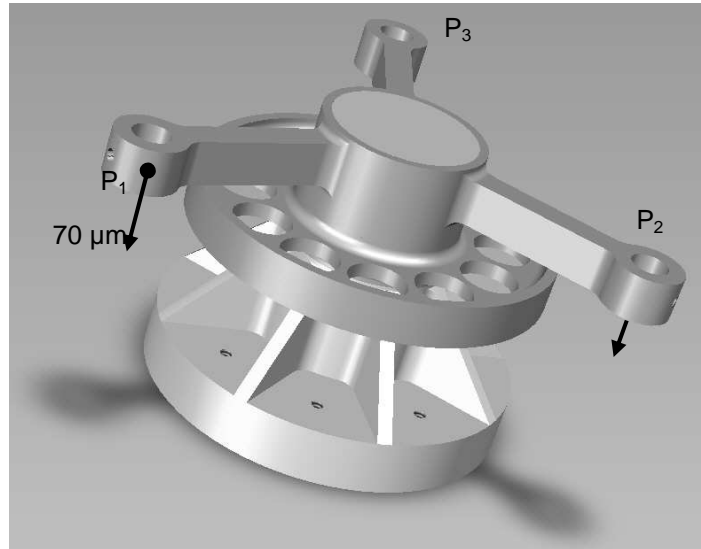


Fig. 7: Upper bearing. It “floats” over the sample. 70  $\mu\text{m}$  are imposed at the level of the  $P_i$  points.

The upper bearing (fig. 7) is literally “floating” on the surface of the concrete. It behaves like a piston inside the mould. Holes through the bearing ensure the bleeding water passing through the bearing. Three LVDT’s can be fixed on the arms placed at  $120^\circ$  around the upper part of the bearing. A ring at mid height ensures the guiding of the bearing inside the mould.

### 2.3 Protocol of loadings

Once the rig is placed between the platens of the testing machine, a few tenths of minutes after casting, a program of cyclic loadings and data processing is started. The period of one cycle is approx. 30 mn. (figure 8). In a first segment of the period (1430 s), no contact exists between the conical upper tool and the upper bearing. An approach is then triggered controlled at a constant displacement rate of the piston of the machine (2<sup>nd</sup> segment). When the rod of the conical tool is in contact of the upper bearing, the control is transferred to the rate of the displacement measured by the LVDT inside the conical tool (3<sup>rd</sup> segment). Progressively, the movement is stopped when the tip of the rod arrives at the level of the bottom surface of the conical tool. Taking the accuracy of the LVDT into account, this position is defined at a few micrometers. At this point, the control is transferred to the mean displacement of the 3 LVDT’s fixed on the arms of the upper bearing (4<sup>th</sup> segment). The rate of displacement is fixed at 0.01 mm/mn. When the displacement reaches 0.07 mm, the ramp is stopped and the control stays still (5<sup>th</sup> segment) on the mean displacement if a relaxation test has to be performed or on the load measurement if a creep test has to be performed. This value of 0.07 mm correspond to a deformation of the sample equal to approx.  $350 \cdot 10^{-6}$ . In compression, it is assumed that no damage is applied to the sample whatever the age is. The plateau controlled in displacement or in load is applied over a period of 5 mn. At the end of the plateau, the sample is unloaded (6<sup>th</sup> segment) to begin the first segment of the next cycle.

As the stiffness of the sample increases, the maximum load at the end of the loading increases under the effect of the imposed displacement (fig. 8) from one cycle to the next one. This displacement should have been constant but variations around the aimed value of 0.07 mm were observed, so that successive peak loads, on the fig. 8 seem to be a little bit scattered. For each cycle, a stiffness is determined which is compared to a F.E. elastic simulation giving a relation between the stiffness and the E-modulus. This method, taking into account the effect of the confinement inside the stainless steel mould, gives the evolution of the Young’s modulus at early age (fig. 9 and 3). The comparison with more classical strain measurement shows a perfect agreement [2]. Creep and relaxation measurements do not need such a calculation to give results. Indeed, the load remains constant or almost constant during the test, so the confinement of the mould is not so involved in the process.

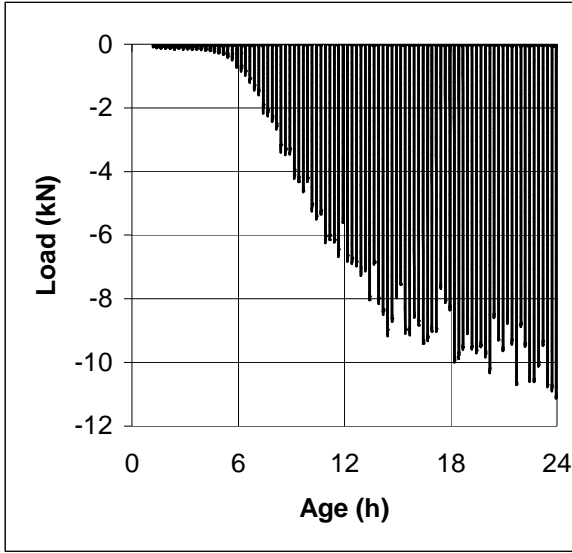


Fig. 8: Monitoring of the load.

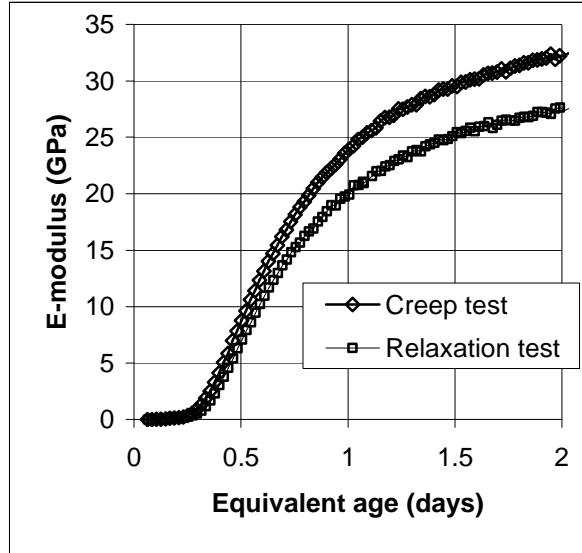


Figure 9 – E-modulus monitoring.

### 3. Results and discussions

One creep test and one relaxation test are presented here. For each test, 96 cycles were triggered every 30 minutes.

#### 3.1 Creep test

A typical creep record is presented in the figure 10. The age of the concrete is called  $t$ . The sample deformation,  $\epsilon(t)$ , is measured continuously. At any cycle, named  $i$ , the creep is counted as soon as the plateau is reached. This moment is called  $t_{0i}$ . The creep is then the difference between  $\epsilon(t)$  and  $\epsilon(t_{0i})$ :  $\epsilon(t, t_{0i}) = \epsilon(t) - \epsilon(t_{0i})$ . The stress reached at the plateau is called  $\sigma_{0i}$ .

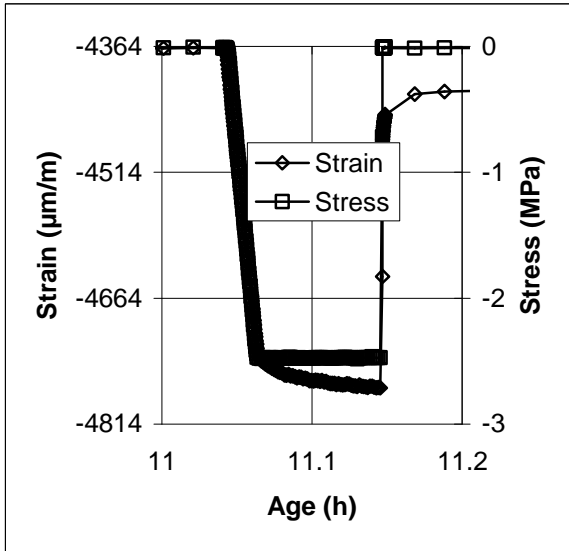


Fig. 10: Typical creep cycle.

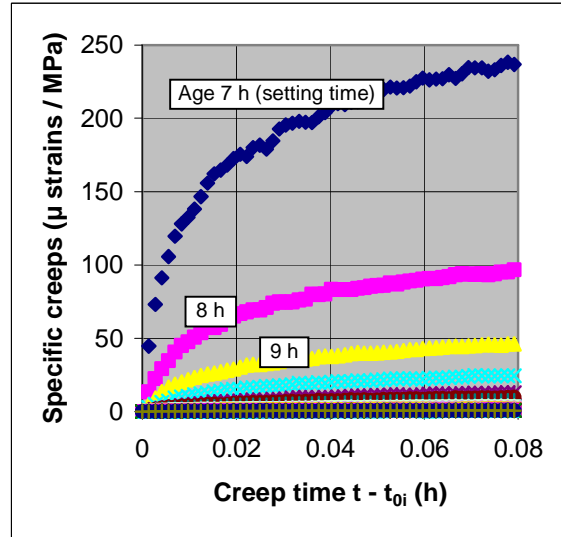


Fig. 11: Specific creeps. Only 48 curves are plotted

For each cycle, the compliance,  $J(t, t_{0i})$ , can be defined as the deformation counted from the beginning of the loading ramp divided by the stress applied during the plateau. Even if there are certainly delayed effects during the loading, the “elastic” part can be removed to obtain the specific creep (fig.11):

$$J^*(t, t_{0i}) = (J(t, t_{0i}) - 1/E_{0i})$$

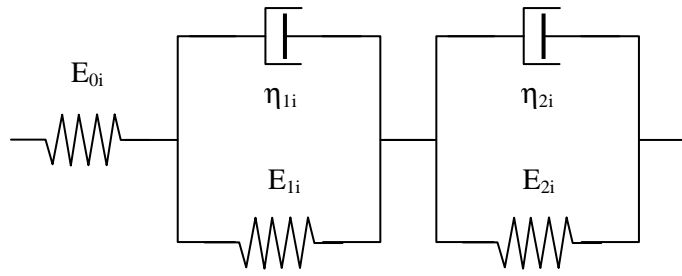


Fig. 12: Dirichlet model

$E_{0i}$  being the E-modulus before the plateau for the cycle  $i$ . It is also assumed that the creep is proportional to the stress.

In order to fit the observed specific creep of each cycle, an uniaxial Dirichlet model (fig. 12) gave the best result on the first cycles analysed.

The response to a sudden loading (compliance in function of the time) of such a model is given by the following expression:

$$J(t, t_{0i}) = \frac{1}{E_{0i}} + \frac{1}{E_{1i}} \left( 1 - \exp\left(-\frac{t - t_{0i}}{\tau_{1i}}\right) \right) + \frac{1}{E_{2i}} \left( 1 - \exp\left(-\frac{t - t_{0i}}{\tau_{2i}}\right) \right) \quad (1)$$

With  $\tau_{1i} = \eta_{1i}/E_{1i}$  et  $\tau_{2i} = \eta_{2i}/E_{2i}$ .

Or, expressed in specific creep, the elastic part is removed:

$$J^*(t, t_{0i}) = J(t, t_{0i}) - \frac{1}{E_{0i}} = \frac{1}{E_{1i}} \left( 1 - \exp\left(-\frac{t - t_{0i}}{\tau_{1i}}\right) \right) + \frac{1}{E_{2i}} \left( 1 - \exp\left(-\frac{t - t_{0i}}{\tau_{2i}}\right) \right) \quad (2)$$

It has been rapidly difficult to fit (identification of the  $E_{1i}$ ,  $E_{2i}$ ,  $\tau_{1i}$  and  $\tau_{2i}$ ) the 96 cycles. That's why it was decided to normalize the specific creep of each cycle by the value reached at the end of the plateau (5 mn) in order to observe an eventual similarity of the curves.

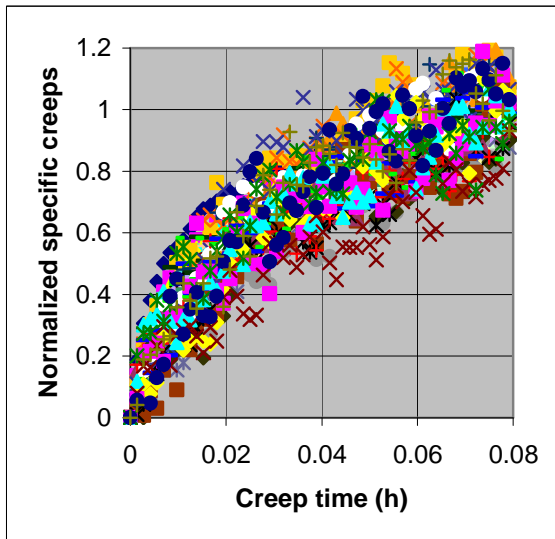


Fig. 13: The specific creeps are normalized by their value at 5 mn.

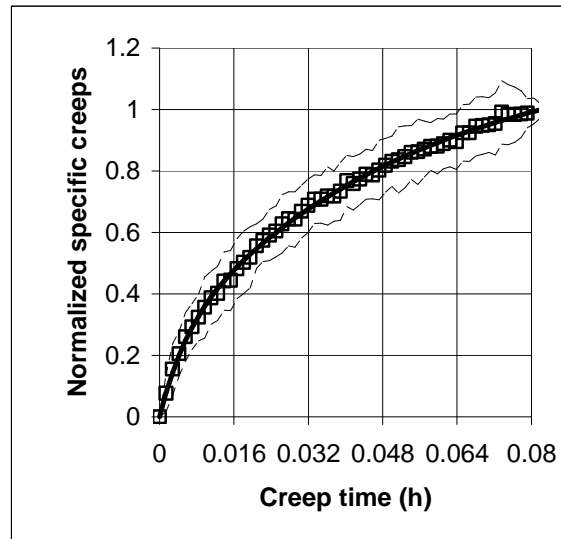


Fig. 14: Mean values of the normalized specific creeps (dots) between  $\pm$  one standard deviation fitted (bold line) by the expression (3).

This new quantity starts at 0 and reach 1 at 5 mn. In that case it is observed that all the cycles are quasi superimposed (fig. 13). On this figure the points seem very scattered but the amplitudes at 5 mn are decreasing sharply with the age and the treatment emphasizes the noise of the measurements for low amplitudes. The mean values and the standard deviations are plotted in the fig. 14.

At this point, it can be observed that all the elementary specific creeps occurring over short periods of 5 mn, have the same kinetic. It means that any elementary specific creep,  $J^*(t, t_{0i})$ , can be modelled by a product of two terms:

- ☞ a dimensionless kinetic term, function of the creep time,  $\Omega(t, t_{0i})$
- ☞ an amplitude, function of the age,  $A_f(t_{0i})$ , expressed here in  $\mu\text{strain}/\text{MPa}$ .

The following expression, built on the model of the expression (2), gives such a product:

$$J^*(t, t_{0i}) = A_f(t_{0i}) \cdot \Omega(t, t_{0i}) = A_f(t_{0i}) \left\{ C_1 \left[ 1 - \exp\left(-\frac{t - t_{0i}}{\tau'_1}\right) \right] + C_2 \left[ 1 - \exp\left(-\frac{t - t_{0i}}{\tau'_2}\right) \right] \right\} \quad (3)$$

By identification:

$$\frac{1}{E_1} = A_f(t_{0i}) C_1 \quad \text{and} \quad \frac{1}{E_2} = A_f(t_{0i}) C_2$$

$$\tau_{11} = \tau'_1 \quad \text{and} \quad \tau_{21} = \tau'_2$$

The dimensionless term of this expression is fitted to the points of the figure 14 (least-squares method) by adjustment of the parameters given in the table 2. The evolution of the amplitude  $A_f(t_{0i})$  is given by the fig. 15..

$C_1$	$C_2$	$\tau'_1$ (h)	$\tau'_2$ (h)
0.966	0.238	0,0528	0,00547

Table 2: Adjusted parameters of the model fitting the mean specific creep in compression.

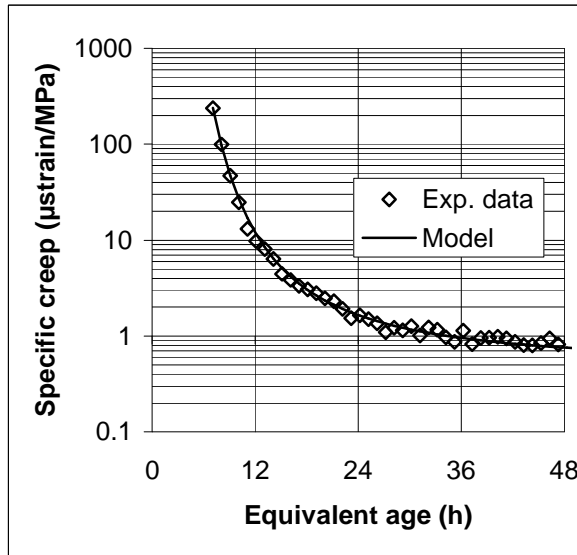


Fig. 15: Amplitude of the specific creep at the end of each cycle (5mn). The experimental data are fitted by the following function:

$$A_f(t_{0i}) = 0.155 \exp(51.98 / t_{0i}) + 0.3$$

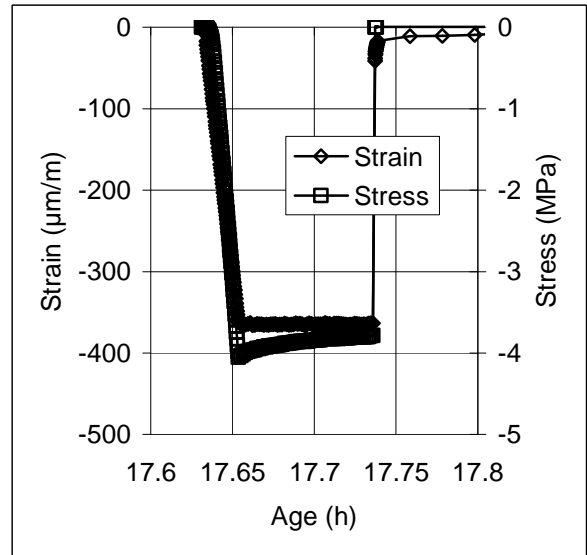


Fig. 16: Typical cycle during a relaxation test.

The characteristic times ( $\tau_{1i}$  and  $\tau_{2i}$ ) and the coefficients ( $C1$  or  $C2$ ) are constant while the stiffness's  $E_1$  and  $E_2$  of equation (2) evolve in function of the term of amplitude:

$$E_1 = \frac{1}{A_f(t_{0i}) C_1} \quad \text{and} \quad E_2 = \frac{1}{A_f(t_{0i}) C_2}$$

These parameters can be easily used in numerical computations.

If the creep has to be rebuilt, a third stress term,  $\sigma_{0i}(t)$ , is included in the product (3) transforming the specific creep in strain:  $J(t, t_{0i}) \cdot \sigma_{0i} = \varepsilon(t, t_{0i})$

It can be verified that this function is in good agreement with any elementary 5 mn creeps over a period of 48 h.

### 3.2 Relaxation test

Concerning the relaxation test, a typical record is presented in fig. 16.

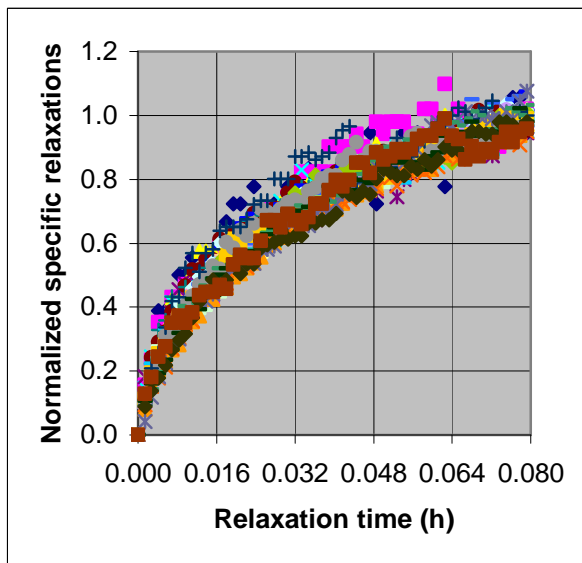


Fig. 17: Specific relaxations normalized by their values at 5 mn.

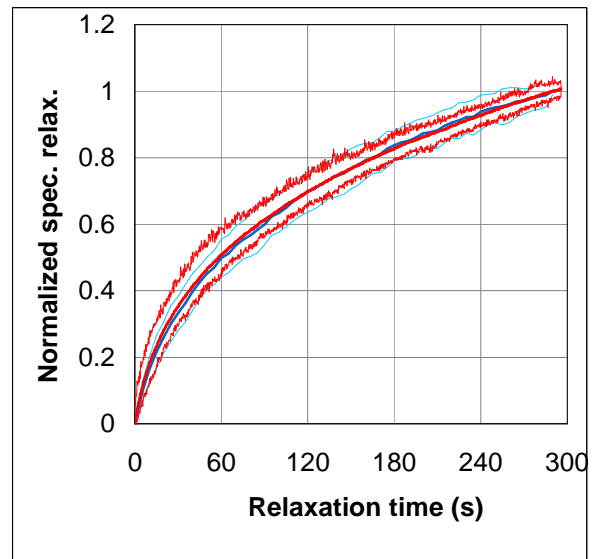


Fig. 18: Mean values of the normalized specific relaxations bordered by  $\pm$  the standard deviation. Both the results obtained by BTJASPE (blue) and the TSTM (in red, see part II) are plotted.

Near the end of the cycle  $i$ , at  $t_{0i}$ , a constant strain  $\varepsilon_{0i}$  is applied and the stress  $\sigma(t, t_{0i})$  is recorded. This strain is considered to be applied instantaneously even if, experimentally, it is applied over a finite period of time. The ratio:  $R(t, t_{0i}) = \sigma(t, t_{0i}) / \varepsilon_{0i}$  is defined as the stiffness. The specific relaxation  $R^*$  is defined as this stiffness diminished of the initial stiffness at  $t_{0i}$ .

$$R^*(t, t_{0i}) = R(t, t_{0i}) - R(t_{0i}, t_{0i}) = R(t, t_{0i}) - E_{0i} \quad (4)$$

As for the creep,  $R^*$  can be normalized by the value reached at the end of the plateau. The whole bunch of recordings is given in the figure 17 while the mean values are plotted in figure 18. In this figure, the results obtained with the TSTM are also plotted. The light lines, in blue or red, represent ranges delimited by  $\pm$  standard deviations. For both the test setups, results are perfectly superimposed. The TSTM experimentations will be developed in the part II.

Again, each individual stress relaxation can be modelled by the product of a unique term giving the kinetic over a period of 5 mn and a term giving the amplitude in function of the age (fig. 19).

It must be underlined that the kinetic dimensionless terms for the relaxation and the creep in compression are perfectly superimposed (fig. 20). The same dimensionless function can be used to fit the kinetics of the elementary creeps or the relaxations in compression at early age as they were experimentally defined in this study. In that case one can use this expression to model the stress relaxation kinetic observed:

$$R^*(t, t_{0i}) = A_r(t_{0i}) \left\{ C_1 \left[ 1 - \exp\left(-\frac{t-t_0}{\tau'_1}\right) \right] + C_2 \left[ 1 - \exp\left(-\frac{t-t_0}{\tau'_2}\right) \right] \right\} \quad (5)$$

The term of amplitude,  $A_r(t_{0i})$ , follows the observation given by the figure 19. The characteristic times ( $\tau'_1$  and  $\tau'_2$ ) are equal to those obtained for the creep test.

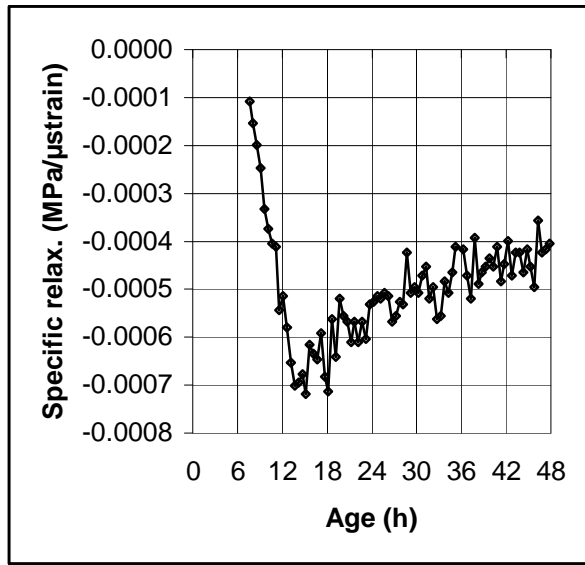


Fig. 19: Amplitude of the specific relaxations,  $A_r(t_{0i})$ , at the end of each cycle (5mn). The absolute value increases until 14.6 h and it decreases after.

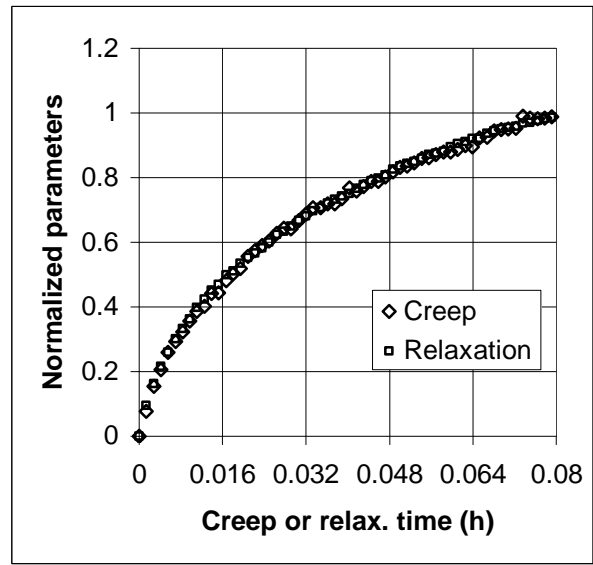


Fig. 20: The normalized specific creep and relaxation (kinetic of the delayed phenomena) in compression are perfectly superimposed.

Finally, a third term (the strain value of the plateaux) allows rebuilding each individual relaxation in compression with a sufficient accuracy.

## 4. Conclusions

A test rig designed for the monitoring of the Young's modulus of a concrete at early age is used for the monitoring of cyclic and short creeps or relaxations. The cycle duration is approx. 30mn. The creep or relaxation duration is 5 mn and the loading duration is 70 seconds. The loading consist in applying a constant strain rate (5  $\mu$ strain/s).

It is observed, for this first approach, that each individual creep or relaxation can be expressed as the product of a dimensionless term describing the kinetic and a term related to the amplitude. The kinetic term is not only the same for each cycle of a single test but it is also the same for creep and relaxation tests.

It is underlined that the loadings are not instantaneous while the model used for the description of the observation is commonly used when the load is applied suddenly. Moreover, this kind of model is adapted for non ageing materials (linear visco-elasticity). More refined descriptions should be used

taking into account the initial ramp. A sudden loading is not realistic even if it can be faster than the one applied for the present test.

More sophisticated loadings mixing tension and compression associated with different plateau duration are still needed for computational purposes.

The effect of the temperature is still to be taken into account. The test rig is designed to control easily the temperature.

The creep recovery measurements together with transverse strains during the creep tests should also be examined in future studies.

The part II will present bidirectional loadings applied on the TSTM. Tensile and compressive loadings are presented and compared to these previous results.

### **Acknowledgements**

Special thanks are addressed to the successive students, Pierre Baesens and Jérôme Carette, from Université Libre de Bruxelles, BATir Department and Pierre Friedrich from Université Paris-Sud11 who worked on the different tests.

### **References**

- [1] Darquennes, A., Staquet, S., Delplancke, M.-P., Espion B., *Effect of autogenous deformation on the cracking risk of slag cement concretes. Cement and Concrete Composites. Volume 33, Issue 3, March 2011, pages 368-379.*
- [2] Boulay C., Merliot E., Staquet S., Marzouk O., *Monitoring of the concrete setting with an automatic method, 13th International Conference Structural Faults & Repair - 2010, Edinburgh, 15-17/6/2010. Proceedings CD ROM (M. FORDE, editor), Engineering Technics Press, Edinburgh, U.K., 11 pp., ISBN 0-947644-67-9. (Book of Abstracts: ISBN 0-947644-66-0; p.98).*
- [3] Morgan P.H., Mercer L.P., Flodin N.W. (1975) *General model for nutritional responses of higher organisms. Proceedings of the National Academy of Sciences of the United States of America.*